

Original Article

Prognostic value and risk model construction of hypoxic stress-related features in predicting gastric cancer

Jiamin Guo¹, Wen Xing², Wei Liu¹, Jing Liu³, Jing Zhang⁴, Zuming Pang³

¹Abdominal Oncology Surgery, Shaanxi Province Cancer Hospital, No. 309, Yanta West Road, Yanta District, Xi'an 710061, Shaanxi, China; ²Internal Medicine, Northwest University Hospital, No. 229 Taibai North Road, Beilin District, Xi'an 710061, Shaanxi, China; ³Department of Gastroenterology, Xianyang First People's Hospital, No. 10, Biyuan Road, Qindu District, Xianyang 712000, Shaanxi, China; ⁴Internal Medicine, Xianyang Hospital of Yan'an University, No. 38 Wenlin Road, Weicheng District, Xianyang 712000, Shaanxi, China

Received September 9, 2022; Accepted November 10, 2022; Epub December 15, 2022; Published December 30, 2022

Abstract: Objective: Hypoxia promotes tumor progression from multiple aspects, including metabolism, proliferation, migration and angiogenesis. Therefore, a thorough understanding of the impact of hypoxia on gastric adenocarcinoma (STAD) is warranted. The aim of the present study was to find a prognostic model of hypoxia in gastric cancer (GC) and its relationship with the immune microenvironment. Methods: Distinct hypoxia-related patterns were identified with an unsupervised consensus clustering algorithm in STAD patients from the Gene Expression Omnibus (GEO) and the cancer genome atlas (TCGA) cohorts. The different biological processes among different hypoxia-related clusters were then explored with the algorithm of single sample gene set enrichment analysis. Then hypoxia-related Hub genes were selected by weighted gene co-expression network analysis (WGCNA) prior to the construction of a hypoxia-related gene prognostic model. The model was constructed using multivariate Cox regression analysis, least absolute shrinkage and selection operator (LASSO) regression and univariate Cox regression analysis. The relationship between immune infiltration and hypoxia-related features was analyzed. Results: We identified a hypoxia-related cluster (magenta) by WGCNA and found that different prognosis can be evidently induced by various hypoxia response patterns. LASSO analysis found seven hypoxia-related genes CPZ, LBH, NOX4, NRP1, NOS3, C3orf36 and CDH6, which were then used for the construction of hypoxia-related gene prognostic model. The model was verified by TCGA database and GEO dataset and showing good prognostic value. Conclusions: A novel hypoxia-related prognostic signature was constructed to predict prognosis and correlate with immune infiltration in STAD. Hypoxia-related prognostic features are expected to be a new prognostic tool for GC.

Keywords: Gastric adenocarcinoma, hypoxia, risk model, LASSO, WGCNA

Introduction

With the improvement of living standards, human dietary structure has changed dramatically, resulting in a surge in the incidence of digestive tract diseases [1]. Data have shown that there are about 1 million patients newly diagnosed with gastric cancer (GC) each year, while more than 780,000 patients die from it each year [2]. Due to the relatively concealed incidence of GC and the low rate of early diagnosis, many patients often miss the chance of surgical treatment due to tumor metastasis at the time of diagnosis [3]. In addition, treatments fail frequently due to the lack of targeted agents and the presence of chemoresistance, which are also the main reasons for the poor progn-

sis of GC patients, with a five-year survival rate of less than 20% [4, 5]. With the continuous improvement of medical care, the survival rate of GC patients has ascended. Unfortunately, the recurrence and metastasis are still main causes of GC-related death [5], and current treatment for those remains unsatisfactory [6]. Studies have reported that immunosuppressive agents have considerable anti-tumor effects and are able to control adverse effects [7, 8]. In addition, it has been shown that PD-L1-positive patients with advanced and metastatic GC are very sensitive to immunotherapy.

Tumor microenvironment refers to the biological environment in which tumors occur, localize and develop [9]. The interaction between the

Prognostic value and risk model construction of hypoxic stress-related features

microenvironment and the tumor has a significant impact on the survival and metastasis of tumor cells [10, 11]. Hypoxia is a major trait of tumor microenvironment, which is caused by the imbalance of oxygen supply and demand because tumor cell proliferation inevitably increases consumption of oxygen [12]. Tumor hypoxia leads to hypoxia-inducible factor (HIF) activation, which mediates gene expression, pH regulation, metabolic pathways, protein synthesis and DNA replication [11]. Therefore, tumor hypoxia not only affects tumor growth and metastasis, but also leads to angiogenesis, genetic instability, heterogeneous changes and resistance to therapy, which are poor prognostic factors for tumor [10]. A growing number of studies have shown that hypoxia is associated with poor prognosis of solid tumors [13]. Given the important role of hypoxia in GC, its detection and assessment are conceivably crucial. Therefore, further studies on the relationship between hypoxia and immunity in GC are needed to develop new therapeutic strategies.

Biological information plays a crucial role in biological research. Being utilized in the field of life sciences, modern industries driven by computers greatly alleviates the labor volume of scientific researchers, simplifies the steps of experimental results processing, and is more accurate in the processing of experimental data [14]. Early studies have found [15] that constructing risk models for related diseases plays a critical role in the prediction and diagnosis of the diseases and provides a new tool for clinical diagnosis and prognosis observation. In this study, we constructed hypoxia-related features by bioinformatics methods and validated hypoxia-related prognostic features using GSE84437 microarray as external data to better demonstrate the relationship between risk score, overall survival (OS) and immune infiltration in GC patients.

Materials and methods

Data collection

The discovery cohort comprised 357 GC patients retrieved from the Gene Expression Omnibus (GEO, <https://www.ncbi.nlm.nih.gov/geo/>) database (GSE84437) [16]. Cancer Genome Atlas (TCGA) [17] cohort contains 407 samples from the “TCGA-STAD” project, including 32 control samples and 375 tumor sam-

ples, with related level 3 gene expression data collected from 11 November 2019, Genomic Data Commons (<https://portal.gdc.cancer.gov>). A total of 314 tumor samples remained after deleting samples with missing data (age, sex, survival time, survival status, T, N, M, clinical stage). Informed consent and Institutional Review Board approval were not entailed for de-identified data analysis from the TCGA and GEO databases. Lima method was used for identification of differential genes. Hypoxia-related differential genes were considered if an FDR-adjusted p -value < 0.05 and an absolute value of \log_2 (fold change) > 1 .

Identification of hypoxia-related genes

By searching MSigDB database [18] hypoxia genome, we found three genomes of M5891, M10508 and M641. A total of 311 hypoxia genes were found by integration.

Weighted correlation network analysis (WGCNA) and feature enrichment analysis

WGCNA R program package was utilized for analyses in the present study [19]. By integrating the content of the TCGA database, 58,938 genes were analyzed for co-expression networks, and 14 co-expression modules were finally obtained. Calculating the correlation between module feature vectors and gene expression sex resulted in MM, we confirmed 652 genes of high connectivity of modules clinically significant as Hub genes according to the cutoff criteria ($|MM| > 0.4$).

Immune infiltration analysis

ESTIMATE [20], the newly developed algorithm (estimating immune and stromal cells expression data in malignant tumor tissues), utilizes features of tumor tissue transcriptome profiles to infer the proportions of different infiltrating stroma and immune cells. ESTIMATE was used in the present study to estimate immune scores to represent immune cell infiltration for immune status prediction in each GC sample. To quantify the immune cell composition of each sample, CIBERSORT software [21] was applied to assess the proportion of immune cells in the GC expression matrix. CIBERSORT, a commonly used tool for characterizing the immune cell composition of complex gene expression profiles [22], was applied to identify immune cell

Prognostic value and risk model construction of hypoxic stress-related features

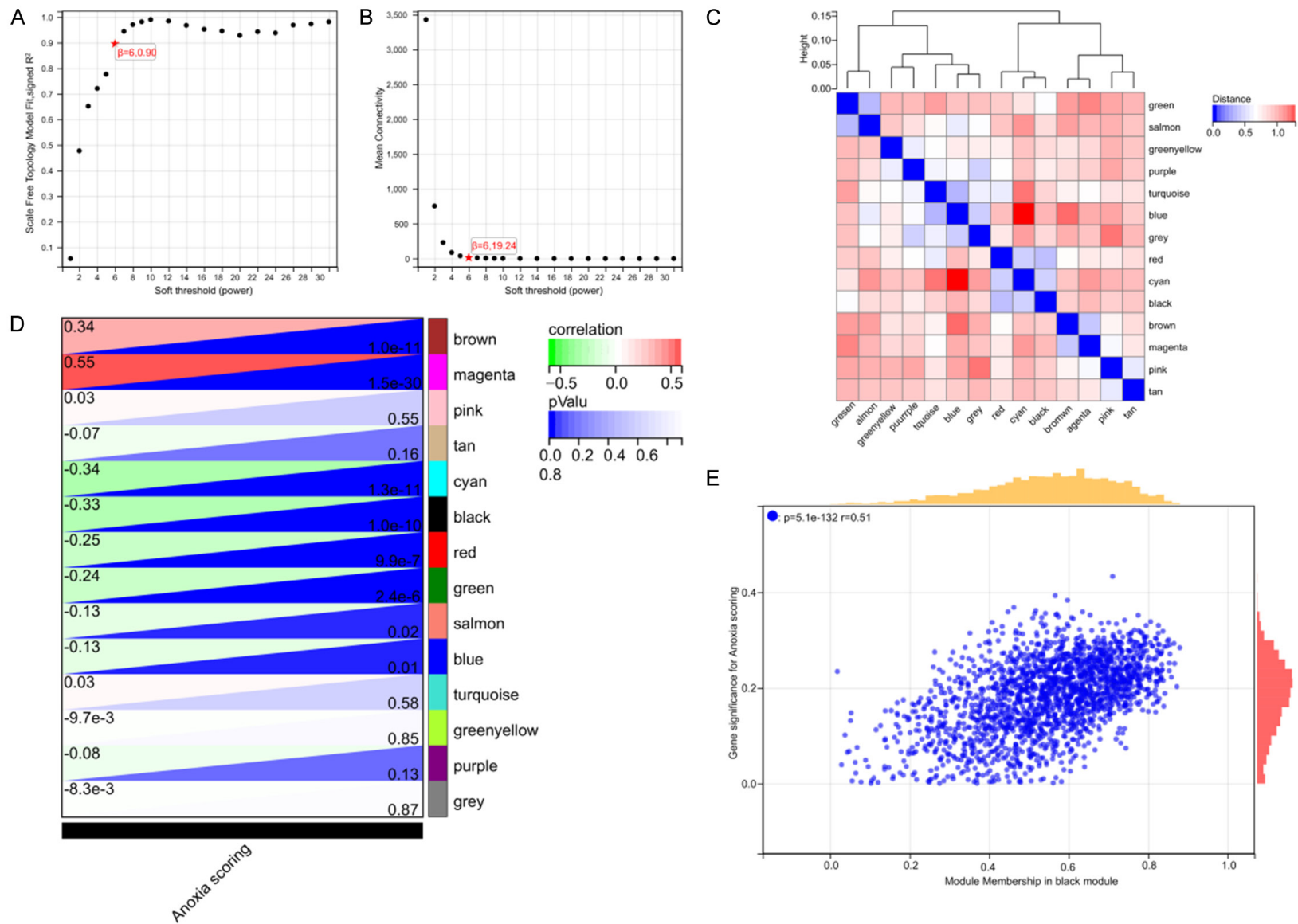


Figure 1. Potential genomes associated with hypoxic stress were analyzed by WGCNA. A. Relationship between scale-free R^2 and soft threshold; B. Relationship between Average Connectivity and Soft Threshold; C. WGCNA won a total of 14 modules; D. Correlation of 14 modules with hypoxic stress-related gene scores after ssGSEA analysis; E. Scatter plot of correlation analysis between magenta module and hypoxic stress-related gene scores. Note: Weighted Gene Co-expression Network Analysis (WGCNA), One Sample Immuno-Infiltrate Analysis (ssGSEA).

Prognostic value and risk model construction of hypoxic stress-related features

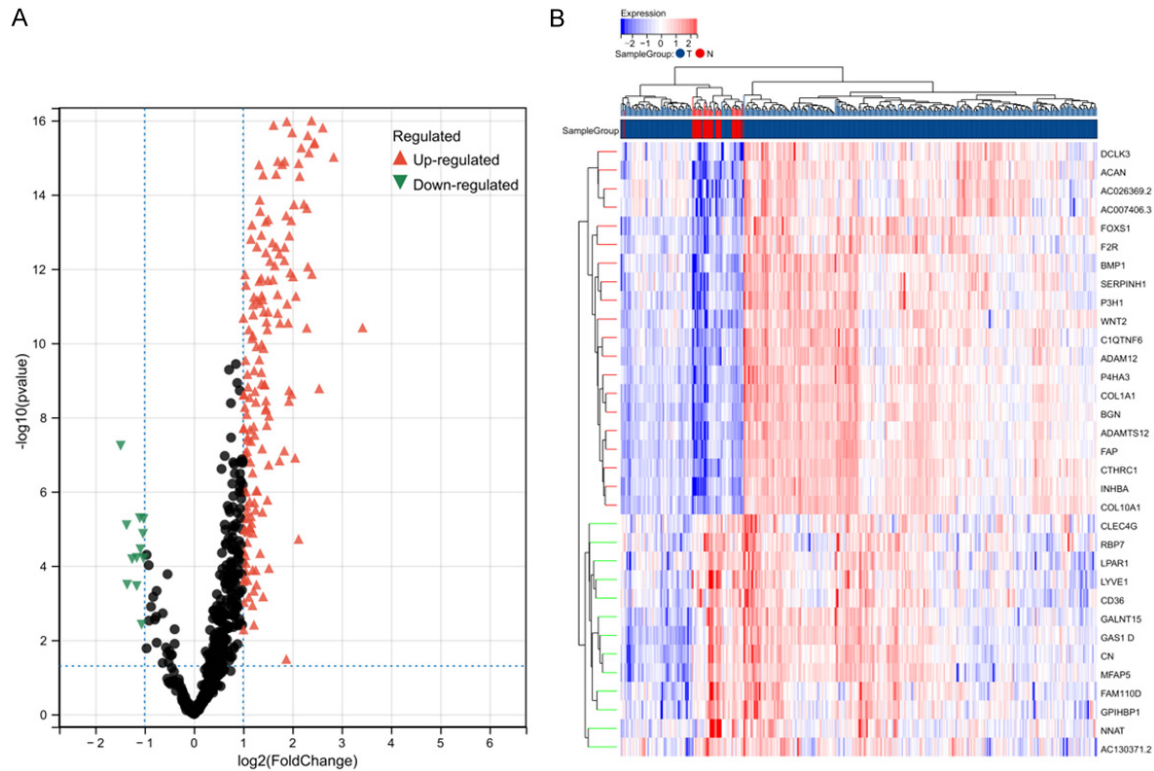


Figure 2. Difference analysis of Hub genes. A. Limma analysis of 652 gene volcano maps; B. Heatmap of Top 20 Differential Genes. Note: Critical genes (Hub genes).

composition in each sample, and $P < 0.05$ was taken as the significant level.

Identification of hypoxia-related gene prognostic markers

Prognostic associated genes were identified based on Cox regression analysis. Afterwards, LASSO Cox regression was conducted to select independent prognostic markers for evaluating OS of GC patients ($P < 0.05$). Risk Score (RS) was calculated by the following formula: Risk scores = $\sum_i^n X_i \times Y_i$. (X_i : coefficient of each gene, Y_i : expression of each gene). According to median score, GC patients in GEO database were grouped into high-risk and low-risk subgroups. Kaplan-Meier survival curve analysis was used to compare the OS between two groups, and time-related ROC was used to assess the predictive value of the gene markers. In addition, the relationship between GC and clinical parameters was assessed.

ROC diagnostic curve and clinical correlation analysis

We conducted analysis on the relationship between risk score, patient clinical data and

survival using ROC. ROC curves were generated with survminer package, survival package, and timeROC package. Among them, timeROC package was used to predict survival in the first, second and third year.

Statistical methods

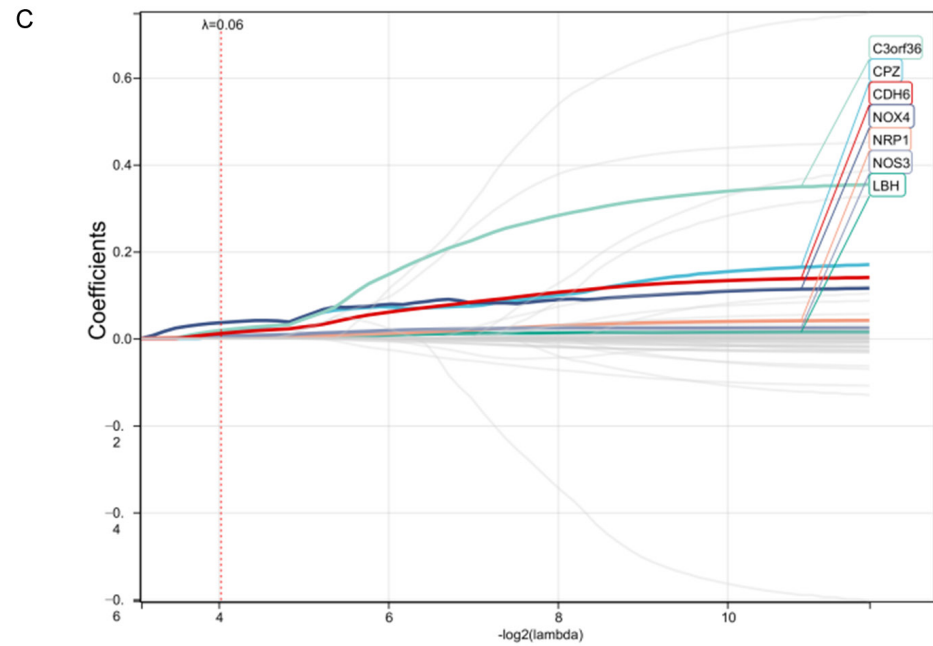
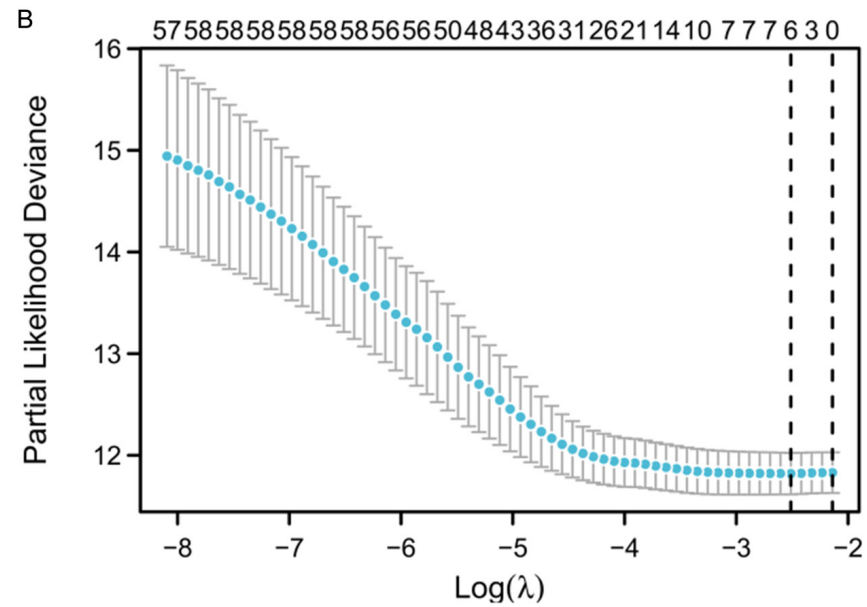
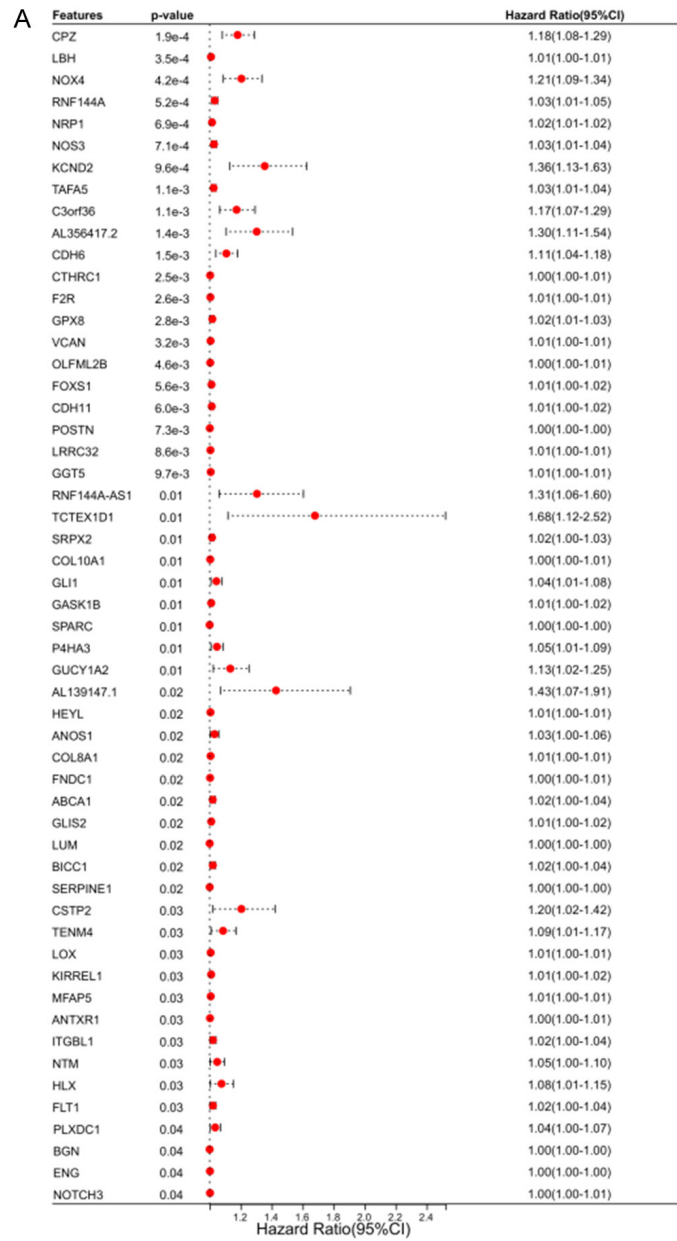
R software (version 4.1; <https://www.r-project.org/>) was utilized for all statistical analyses. Wilcoxon's test was used for pairwise comparisons. Comparisons of OS were conducted by survival and the survminer R package with Kaplan-Meier curves of the log-rank test. A statistical difference was taken when $P < 0.05$.

Results

WGCNA and key module identification

Three genomes M5891, M10508 and M641 were found by searching the MSigDB database for hypoxic genomes, and 311 hypoxia genes by integration. The scores of hypoxia stress genes were obtained by analyzing the scores of 311 hypoxia genes in TCGA-STAD samples using single sample gene set enrichment analysis (ssGSEA). A matrix of 375 TCGA-STAD sam-

Prognostic value and risk model construction of hypoxic stress-related features



Prognostic value and risk model construction of hypoxic stress-related features

Figure 3. Prognostic analysis of hypoxia-related genes. A. Survival analysis of 378 Hub genes in STAD patients using univariate Cox regression; B, C. Coefficient distribution for Cox regression analysis with LASSO, and the calculation of the tuning parameter (λ) based on the partial likelihood bias of 10-fold cross-validation. Note: Critical genes (Hub genes), gastric adenocarcinoma (STAD), Least Absolute Shrinkage and Selection Operator (LASSO).

ples with data was used for WGCNA analysis. A total of 14 modules were obtained after analysis (**Figure 1A-C**). The correlation between modules and hypoxic stress gene scores was analyzed by Pearson test, and there was an evident correlation between magenta module and the score (**Figure 1D, 1E**).

Differential analysis of Hub gene

With the MM threshold of 0.4, the GS threshold of 0.1, the weight threshold of 0.1, the Hub genes in magenta were extracted, and a total of 652 genes were obtained. To further understand the value of Hub gene in GC, we carried out differential analysis on the 652 genes obtained. Through limma analysis ($P < 0.05$, $\log FC = 1$), we obtained a total of 378 differential genes. Among them, there were 353 high-expressed genes and 25 low-expressed genes (**Figure 2A, 2B**).

Prognosis of hypoxia-related genes

To further comprehend the post-value of hypoxia-related genes in STAD patients, we first performed univariate Cox and LASSO regression analysis on the 378 Hub genes after differential analysis. In single factor, we found 54 genes associated with STAD prognosis (**Figure 3A**). Then, by LASSO regression, the genes CPZ, LBH, NOX4, NRP1, NOS3, C3orf36 and CDH6 were found to be correlated with STAD prognosis (**Figure 3B, 3C**).

Construction and validation of hypoxia-related gene signatures

Based on the 7 hypoxia-related genes we found, the coefficient calculation formula was obtained using the LASSO algorithm according to the TCGA cohort risk score: Risk Score = $0.00971480914901194 * CPZ + 0.0021059895241986 * LBH + 0.0363619594442472 * NOX4 + 0.00283696190155081 * NRP1 + 0.00519489735745231 * NOS3 + 0.0187983685058255 * C3orf36 + 0.0114926397607483 * CDH6$. Afterwards, patients were categorized into low-risk and high-risk group according to their median risk scores (**Figure 4A**). In

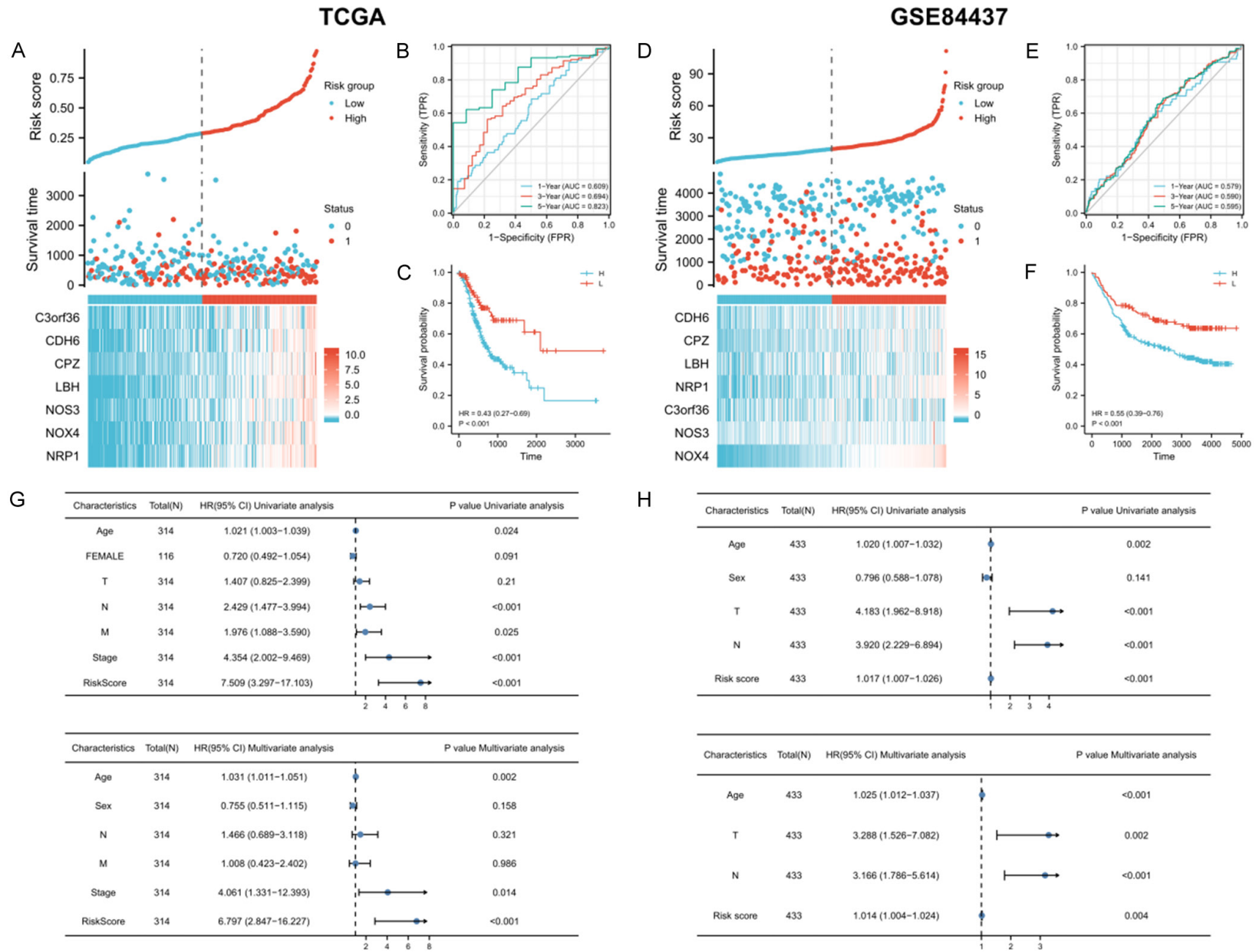
addition, the sensitivity and specificity of the model for predicting the OS of patients were validated by applying ROC curve. We found that this risk model had good accuracy in predicting the 1-year (AUC = 0.72), 3-year (AUC = 0.80) and 5-year (AUC = 0.90) postoperative survival (**Figure 4B**). Kaplan-Meier survival analysis suggested that the Low-risk group held evidently longer OS than its counterpart ($P < 0.001$, **Figure 4C**). This suggested that our model had certain accuracy in predicting the survival and prognosis of STAD patients.

In attempts to verify the generalization of the model, we used an external dataset (GSE-84437) for validation. Based on the risk score calculated from the risk model, patients were ranked from low to high, and the median value was taken to divide patients into high-risk group and low-risk group (**Figure 4D**). Furthermore, the specificity and sensitivity of the model for predicting OS in patients was validated by ROC curve, which we analyzed to further validate the accuracy of the risk scoring model (**Figure 4E**). Survival was worse in the high-risk group and better in its counterpart ($P < 0.001$, **Figure 4F**). Moreover, we regressed the factors affecting patient prognosis in the two datasets by Cox regression analysis, and it was suggested that the risk score was associated with the prognosis of STAD and was an independent factor affecting the prognosis of patients (**Figure 4G, 4H**).

Correlation analysis of risk score based on risk model in pathological data of patients

We also identified the relationship between risk scores and patient pathology data. In our results, patients with lower clinical stage (stage I) had evidently lower risk scores compared to those with high clinical stage (stages II, III, IV) (**Figure 5A**), and patients with T1-T2 stages had significantly lower risk scores than patients with T3-T4 stages (**Figure 5B**). However, there was no difference identified regarding risk scores between patients in N and M stage (**Figure 5C, 5D**), suggesting that our risk score may have high clinical value in predicting the clinical stage of patients.

Prognostic value and risk model construction of hypoxic stress-related features



Prognostic value and risk model construction of hypoxic stress-related features

Figure 4. Construction and validation of the prognostic signature of hypoxia-related genes in TCGA and GSE84437 datasets. (A) Risk score, OS, OS distribution and heatmap of 7 hypoxia-related genes in the TCGA dataset; (B) ROC curves of risk score predicting patient 1-, 3- and 5-year survival in TCGA dataset; (C) Survival in high-risk versus low-risk patients in the TCGA dataset; (D) Risk score, OS, OS distribution and heatmap of 7 hypoxia-related genes in the GEO dataset; (E) ROC curves of risk score predicting patient 1-, 3- and 5-year survival in GEO dataset; (F) Survival of high- versus low-risk patients in (F) GEO Dataset; (G) Relationship analysis between patient risk score and OS in the TCGA dataset by Cox regression; (H) Relationship analysis between patient risk score and OS in the GEO dataset by Cox regression. Note: The Cancer Genome Atlas (TCGA), Gene Expression Omnibus (GEO), Receiver Operating Curve (ROC), Overall Survival (OS).

Immune cell infiltration in different hypoxic states in STAD

Previous studies have shown that hypoxia was an important feature during tumor progression with the ability to modulate tumor immune responses. The StromalScore, ImmuneScore and ESTIMATEScore were obtained by ESTIMATE algorithm, which revealed that ImmuneScore, StromalScore and ESTIMATEScore were evidently increased in the high-risk group compared with those in the low-risk group ($P < 0.001$, **Figure 6A**). Furthermore, CIBERSORTx algorithm was utilized to RNA-seq data, and the abundance of 22 infiltrating immune cells was obtained. Results revealed significant differences between the two groups of patients. Compared with the low-risk group, the abundance of Dendritic cells activated in the high-risk group was evidently higher, while that of Macrophages M2 in the high-risk group was markedly lower ($P < 0.05$, **Figure 6B**).

Discussion

Previous report showed [23] that a risk model for predicting the prognosis of triple-negative breast cancer was successfully constructed by analyzing the characteristics of 21 hypoxia-related genes. It provides a basis for prognosis prediction, risk stratification and personalized treatment for triple-negative breast cancer. Other study has also revealed hypoxia-related signatures (PDSS1, CDCA8, and SLC7A11) to be potential biomarkers for HCC diagnosis, prognosis and recurrence, providing an immunological perspective for the development of personalized therapy [24]. In this study, we also explored the hypoxia signature of STAD and constructed a hypoxia-related prognostic risk score to confirm the relationship between hypoxia and genetic alterations, tumor micro-environment, and immunotherapy.

We identified a total of 54 differential genes associated with the prognosis of patients, and

7 prognostic genes (CPZ, LBH, NOX4, NRP1, NOS3, C3orf36 and CDH6) were identified as components of risk characteristics by Lasso regression. Among them, four genes have been found to be related to GC. NOX4 is considered to be related to GC proliferation and drug resistance. By targeting NOX4, cocoa can block GC cell proliferation [25]. Previous study revealed that [26] overexpression of NOX4 could promote the resistance of GC cells to 5-fluorouracil. NRP1 can be involved in several different types of signaling pathways that control cell migration. A lot of literature has reported that inhibiting NRP1 expression by regulating NRP1 upstream target genes markedly inhibits the growth and metastasis of GC [27]. In the study of Zou et al. [28], it was reported that NOS3 was highly expressed in GC and is an independent prognostic factor for STAD. Their drug response analysis report indicated that NOS3 was inhibited in GC patients after treatment, suggesting that NOS3 may be a new target for GC treatment. Research has also shown that [29] CDH6 is up-regulated in GC, and its high expression indicates that the proportion of patients with T stage was relatively large, and usually with poor prognosis. However, CPZ, LBH and C3orf36 are less studied in GC. By and large, these results suggested that our research protocol can identify novel oncogenic-related genes that are potential therapeutic targets.

To further identify the relationship between the seven prognostic genes and STAD, we grouped patients into low-risk and high-risk groups according to risk scores. Risk signatures based on 7 prognostic genes performed well in the stratification of major STAD risk groups in the TCGA and GEO datasets, as confirmed by ROC curve, KM curve and risk map analysis. Furthermore, we found that prognostic features regarding 3- and 5-year survival showed comparable accuracy in both external (GEO) and internal (TCGA) validation cohorts. Not only that, we found that risk score was a risk factor

Prognostic value and risk model construction of hypoxic stress-related features

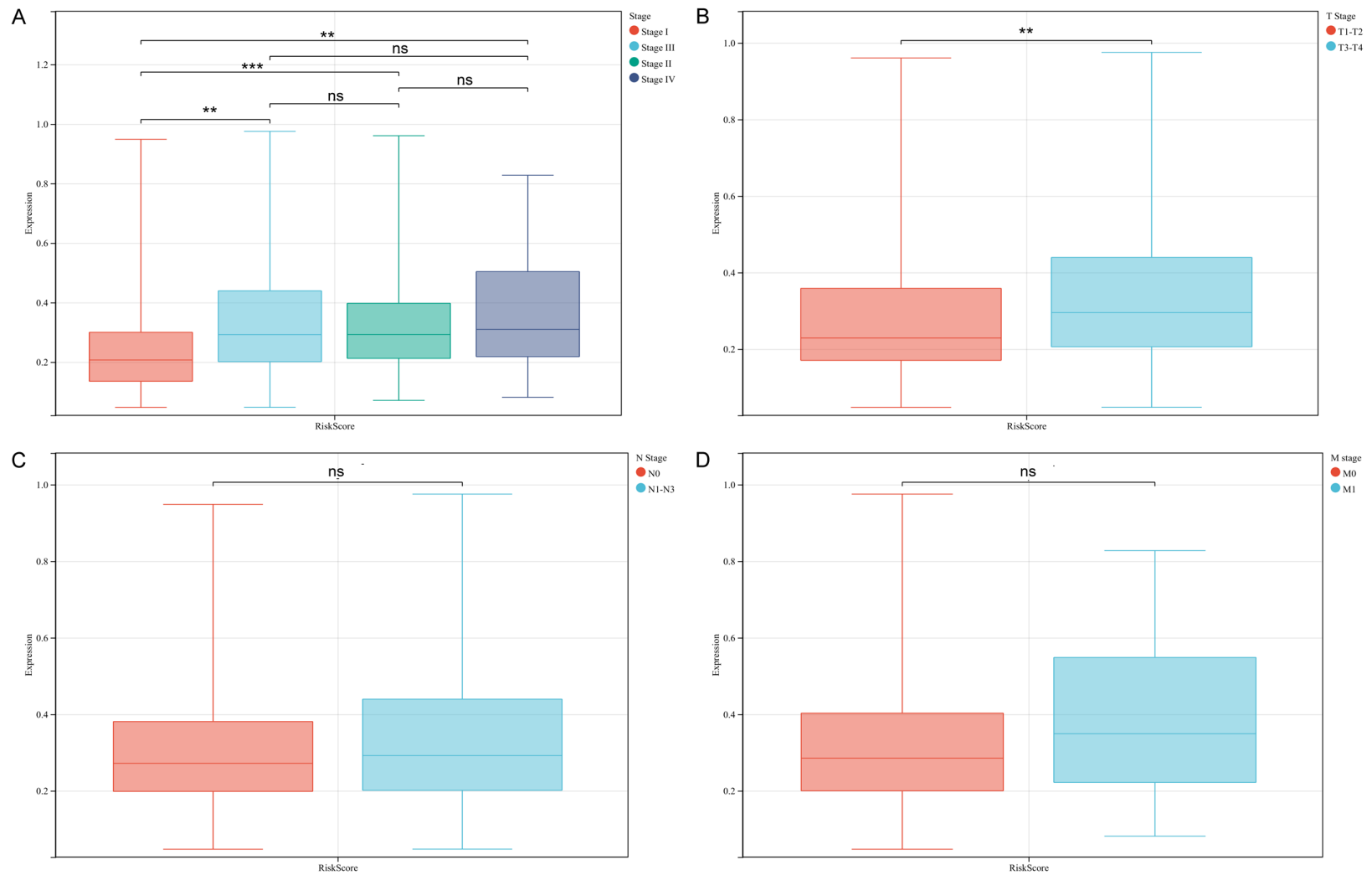


Figure 5. Relationship between risk score and patient pathological data. A. Risk score expression in patients with stage I, II, III and IV; B. Expression of risk scores in patients with T1-T2 and T3-T4; C. Expression of risk scores in patients with N0 and N1-N3; D. Expression of risk scores in patients with M0 and M1. Note: ns indicates that there is no difference between the two groups; * indicates $P < 0.05$ for inter-group comparison; ** indicates $P < 0.01$ for inter-group comparison.

suggesting that the risk model constructed in present study can predict the immune microenvironment effectively.

However, our study has several limitations that need to be addressed. First, as a credit analysis, we did not verify our results through clinical data. Second, there is an absence of disease-free survival data in this study, so the relationship between disease-free survival and the risk model could not be analyzed. Therefore, it is reasonable to validate the STAD risk stratification and prognostic model with more factors and data.

Taken together, a hypoxia-related prognostic signature associated with STAD was identified by our study, which can be used to predict patient survival and is associated with immune infiltration. It is expected to be a potential regimen for clinical STAD treatment and prognosis prediction.

Disclosure of conflict of interest

None.

Address correspondence to: Zuming Pang, Department of Gastroenterology, Xianyang First People's Hospital, No. 10, Biyuan Road, Qindu District, Xianyang 712000, Shaanxi, China. E-mail: pangming118@126.com

References

- [1] Poblocki J, Jasinska A, Syrenicz A, Andrysiak-Mamos E and Szczuko M. The neuroendocrine neoplasms of the digestive tract: diagnosis, treatment and nutrition. *Nutrients* 2020; 12: 1437.
- [2] Bray F, Ferlay J, Soerjomataram I, Siegel RL, Torre LA and Jemal A. Global cancer statistics 2018: GLOBOCAN estimates of incidence and mortality worldwide for 36 cancers in 185 countries. *CA Cancer J Clin* 2018; 68: 394-424.
- [3] Sexton RE, Al Hallak MN, Diab M and Azmi AS. Gastric cancer: a comprehensive review of current and future treatment strategies. *Cancer Metastasis Rev* 2020; 39: 1179-1203.
- [4] Song Z, Wu Y, Yang J, Yang D and Fang X. Progress in the treatment of advanced gastric cancer. *Tumour Biol* 2017; 39: 10104283177-14626.
- [5] Tan Z. Recent advances in the surgical treatment of advanced gastric cancer: a review. *Med Sci Monit* 2019; 25: 3537-3541.
- [6] Zeng D, Wu J, Luo H, Li Y, Xiao J, Peng J, Ye Z, Zhou R, Yu Y, Wang G, Huang N, Wu J, Rong X, Sun L, Sun H, Qiu W, Xue Y, Bin J, Liao Y, Li N, Shi M, Kim KM and Liao W. Tumor microenvironment evaluation promotes precise checkpoint immunotherapy of advanced gastric cancer. *J Immunother Cancer* 2021; 9: e002467.
- [7] Li K, Zhang A, Li X, Zhang H and Zhao L. Advances in clinical immunotherapy for gastric cancer. *Biochim Biophys Acta Rev Cancer* 2021; 1876: 188615.
- [8] Gu L, Chen M, Guo D, Zhu H, Zhang W, Pan J, Zhong X, Li X, Qian H and Wang X. PD-L1 and gastric cancer prognosis: a systematic review and meta-analysis. *PLoS One* 2017; 12: e0182692.
- [9] Arneth B. Tumor microenvironment. *Medicina (Kaunas)* 2019; 56: 15.
- [10] Wu T and Dai Y. Tumor microenvironment and therapeutic response. *Cancer Lett* 2017; 387: 61-68.
- [11] Vitale I, Manic G, Coussens LM, Kroemer G and Galluzzi L. Macrophages and metabolism in the tumor microenvironment. *Cell Metab* 2019; 30: 36-50.
- [12] Jing X, Yang F, Shao C, Wei K, Xie M, Shen H and Shu Y. Role of hypoxia in cancer therapy by regulating the tumor microenvironment. *Mol Cancer* 2019; 18: 157.
- [13] Boutilier AJ and ElSawa SF. Macrophage polarization states in the tumor microenvironment. *Int J Mol Sci* 2021; 22: 6995.
- [14] Chen C, Hou J, Tanner JJ and Cheng J. Bioinformatics methods for mass spectrometry-based proteomics data analysis. *Int J Mol Sci* 2020; 21: 2873.
- [15] Long J, Wang A, Bai Y, Lin J, Yang X, Wang D, Yang X, Jiang Y and Zhao H. Development and validation of a TP53-associated immune prognostic model for hepatocellular carcinoma. *EBioMedicine* 2019; 42: 363-374.
- [16] Barrett T, Wilhite SE, Ledoux P, Evangelista C, Kim IF, Tomashevsky M, Marshall KA, Phillippy KH, Sherman PM, Holko M, Yefanov A, Lee H, Zhang N, Robertson CL, Serova N, Davis S and Soboleva A. NCBI GEO: archive for functional genomics data sets-update. *Nucleic Acids Res* 2013; 41: D991-995.
- [17] Blum A, Wang P and Zenklusen JC. SnapShot: TCGA-analyzed tumors. *Cell* 2018; 173: 530.
- [18] Liberzon A, Birger C, Thorvaldsdottir H, Ghandi M, Mesirov JP and Tamayo P. The molecular signatures database (MSigDB) hallmark gene set collection. *Cell Syst* 2015; 1: 417-425.
- [19] Langfelder P and Horvath S. WGCNA: an R package for weighted correlation network analysis. *BMC Bioinformatics* 2008; 9: 559.
- [20] Yoshihara K, Shahmoradgoli M, Martinez E, Vegesna R, Kim H, Torres-Garcia W, Trevino V,

Prognostic value and risk model construction of hypoxic stress-related features

- Shen H, Laird PW, Levine DA, Carter SL, Getz G, Stemke-Hale K, Mills GB and Verhaak RG. Inferring tumour purity and stromal and immune cell admixture from expression data. *Nat Commun* 2013; 4: 2612.
- [21] Chen B, Khodadoust MS, Liu CL, Newman AM and Alizadeh AA. Profiling tumor infiltrating immune cells with CIBERSORT. *Methods Mol Biol* 2018; 1711: 243-259.
- [22] Zhang B, Tang B, Gao J, Li J, Kong L and Qin L. A hypoxia-related signature for clinically predicting diagnosis, prognosis and immune microenvironment of hepatocellular carcinoma patients. *J Transl Med* 2020; 18: 342.
- [23] Yang X, Weng X, Yang Y, Zhang M, Xiu Y, Peng W, Liao X, Xu M, Sun Y and Liu X. A combined hypoxia and immune gene signature for predicting survival and risk stratification in triple-negative breast cancer. *Aging (Albany NY)* 2021; 13: 19486-19509.
- [24] Tang CT, Lin XL, Wu S, Liang Q, Yang L, Gao YJ and Ge ZZ. NOX4-driven ROS formation regulates proliferation and apoptosis of gastric cancer cells through the GLI1 pathway. *Cell Signal* 2018; 46: 52-63.
- [25] Qin Y, Ma X, Guo C, Cai S, Ma H and Zhao L. MeCP2 confers 5-fluorouracil resistance in gastric cancer via upregulating the NOX4/PKM2 pathway. *Cancer Cell Int* 2022; 22: 86.
- [26] Mei B, Chen J, Yang N and Peng Y. The regulatory mechanism and biological significance of the Snail-miR590-VEGFR-NRP1 axis in the angiogenesis, growth and metastasis of gastric cancer. *Cell Death Dis* 2020; 11: 241.
- [27] Pang W, Zhai M, Wang Y and Li Z. Long noncoding RNA SNHG16 silencing inhibits the aggressiveness of gastric cancer via upregulation of microRNA-628-3p and consequent decrease of NRP1. *Cancer Manag Res* 2019; 11: 7263-7277.
- [28] Zou D, Li Z, Lv F, Yang Y, Yang C, Song J, Chen Y, Jin Z, Zhou J, Jiang Y, Ma Y, Jing Z, Tang Y and Zhang Y. Pan-cancer analysis of NOS3 identifies its expression and clinical relevance in gastric cancer. *Front Oncol* 2021; 11: 592761.
- [29] Zhao Z, Li S, Li S, Wang J, Lin H and Fu W. High expression of oncogene cadherin-6 correlates with tumor progression and a poor prognosis in gastric cancer. *Cancer Cell Int* 2021; 21: 493.
- [30] Mayer A and Vaupel P. Multiparametric analysis of the tumor microenvironment: hypoxia markers and beyond. *Adv Exp Med Biol* 2017; 977: 101-107.
- [31] Wei X, Chen Y, Jiang X, Peng M, Liu Y, Mo Y, Ren D, Hua Y, Yu B, Zhou Y, Liao Q, Wang H, Xiang B, Zhou M, Li X, Li G, Li Y, Xiong W and Zeng Z. Mechanisms of vasculogenic mimicry in hypoxic tumor microenvironments. *Mol Cancer* 2021; 20: 7.
- [32] Hajizadeh F, Okoye I, Esmaily M, Ghasemi Chaleshtari M, Masjedi A, Azizi G, Irandoust M, Ghalamfarsa G and Jadidi-Niaragh F. Hypoxia inducible factors in the tumor microenvironment as therapeutic targets of cancer stem cells. *Life Sci* 2019; 237: 116952.